Text DR1. Radiocarbon Dating – Prior to submission for the AMS radiocarbon analysis, samples were sonicated and rinsed in reagent-grade H_2O and ~30% of the sample mass was removed with 2 M HCl. Radiocarbon ages were converted to calendar years using OxCal 4.2 (Bronk Ramsey, 2009), Marine13 data (Reimer et al., 2013), and a constant regional marine reservoir correction (ΔR; see Tables DR1, DR2, and DR3 for additional details). ΔR value of 5 ± 32 yrs, a weighted mean of eight pre-bomb ΔR values from Florida and Bahamas (see Table DR1), was used for age calibration. For specimens younger than 1950 AD, the fraction of modern carbon ($F^{14}C$) was converted to calendar ages using a regional marine calibration curve and the calibration software OxCal v4.2. The post-1950 regional marine curve was constructed using regional ^{14}C data for corals, surface sea-waters, known-age fish otoliths, and live-collected shells of the bivalve *Transennella* sp. (for details see Tables DR1, DR2, and DR3). All calibrated ages are reported in calendar years relative to 2016 AD, the year of sample collection (2016 AD = 0 yrs). The results are the same for any year zero (e.g., 1950 AD), but the collection date is the most relevant baseline for taphonomic processes. Uncalibrated radiocarbon ages are reported in yrs or kyrs BP, where 0 BP=1950 AD.

Table DR1 – Regional pre-bomb ΔR values for our study site (Bahamas). These pre-bomb ΔR values, listed in the Online Marine Reservoir Correction Database (http://calib.org/marine/), were used for the calculation of a weighted mean ΔR value of 5 ± 32 ^{14}C yr (n=8).

	Location	Latitude	Longitude	Year of collection/ formation	ΔR ± 1σ (^{14}C yr)	References
1	Pickles Reef, Florida	24.9824	-80.4158	AD 1950	-11 ± 26	Druffel (1997)
2	The Rocks, Florida	24.9429	-80.5573	AD 1950	-32 ± 59	Druffel and Linick (1978)
3	The Rocks, Florida	24.9429	-80.5573	AD 1950	-3 ± 23	Druffel (1997)
4	The Rocks, Florida	24.9429	-80.5573	AD 1945	11 ± 24	Druffel (1997)
5	The Rocks, Florida	24.9429	-80.5573	AD 1940	14 ± 21	Druffel (1997)
6	Golding Cay, Bahamas	24.23	-77.62	AD 1912	146 ± 66	Lighty et al. (1982)
7	Bahama Islands	26	-78	AD 1950	-40 ± 42	Broecker and Olson (1961)
8	Bahama Islands	26	-78	AD 1885	56 ± 59	Broecker and Olson (1961)

Table DR2 – ^{14}C values of live-collected shells (*Transenella* spp.) measured in this study. These four shell samples were converted to graphite and measured using the STAR AMS Facility at ANSTO (Fink et al., 2004).

	Location	Lab ID	Sample ID	Year of collection	$F^{14}C$ ± 1σ
1	San Salvador Island, The Bahamas	OZV181	USN30-002	2014	1.0183 ± 0.0035
2	Waccassasa Estuary, Gulf of Mexico	OZV183	003	2016	0.9817 ± 0.0021
3		OZV184	004	2016	0.9816 ± 0.0025
4		OZV185	005	2016	0.9860 ± 0.0024

Table DR3 - Data used to construct the post-1950 regional marine ^{14}C curve used to calibrate the post-bomb ages.

Dataset	**Reference**
Corals for 1951 - 1983	Druffel, 1982, 1989
Surface sea-water collected in August 1992	Severinghaus et al., 1996
Known-age fish otoliths for 1989 and 1996	Baker and Wilson, 2001
Live-collected shells of the bivalve *Transennella* spp.	this study (Table DR2)

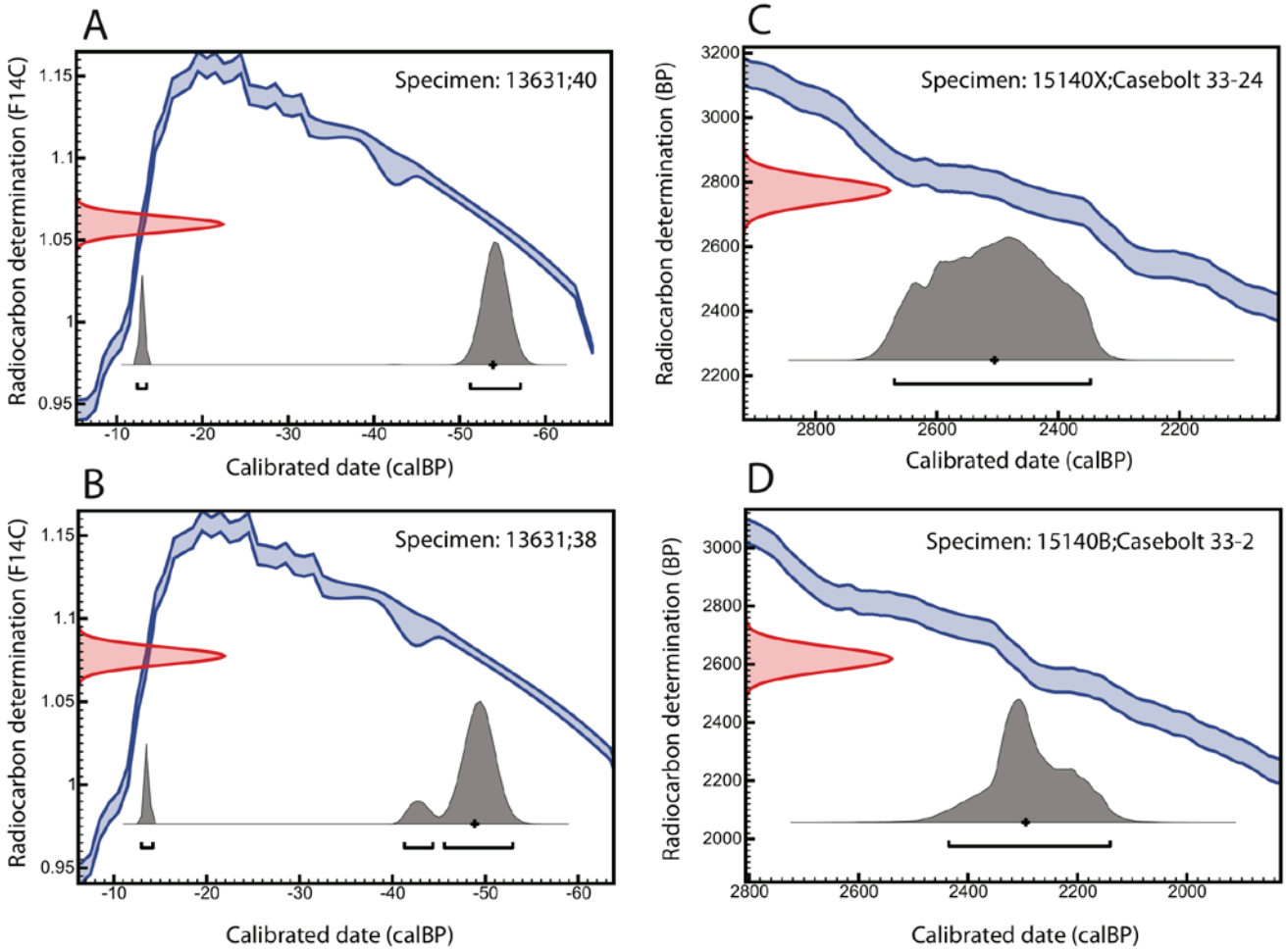

Figure DR1 - Graphical examples of deriving posterior distributions for four radiocarbon-dated specimens. The initial radiocarbon determination (y-axis) includes Poisson distributed measurement error (pink distributions). This measurement uncertainty is translated via the calibration curve (blue curve) to produce posterior distributions of calibrated ages: "specimen posteriors" (grey distributions). Medians of posterior distributions (black crosses) are used as best estimates of actual specimen ages. Black bars beneath specimen posteriors depict calibrated age ranges at 95.4% probability **A.** A post-bomb specimen with the posterior distribution showing a radiocarbon age determination with two alternative distinct age modes due to the non-monotonic trend of the calibration curve (see DR3 for data used to construct the $F^{14}C$ calibration curve). In this case each of the individual age possibilities are symmetrical and unimodal because the respective segments of the calibration curve are linear. **B.** A post-bomb specimen, with a posterior distribution characterized by three distinct modes due to irregularities in the calibration curve (see DR3 for data used to construct the $F^{14}C$ calibration curve). **C.** A pre-bomb specimen with a standard radiocarbon calibration that due to the gentle slope of the Marine13 calibration curve (Reimer et al., 2013) results in a relatively wide and flat calibrated age uncertainty. **D.** A pre-bomb specimen with a standard radiocarbon calibration resulting in an irregular posterior distribution.

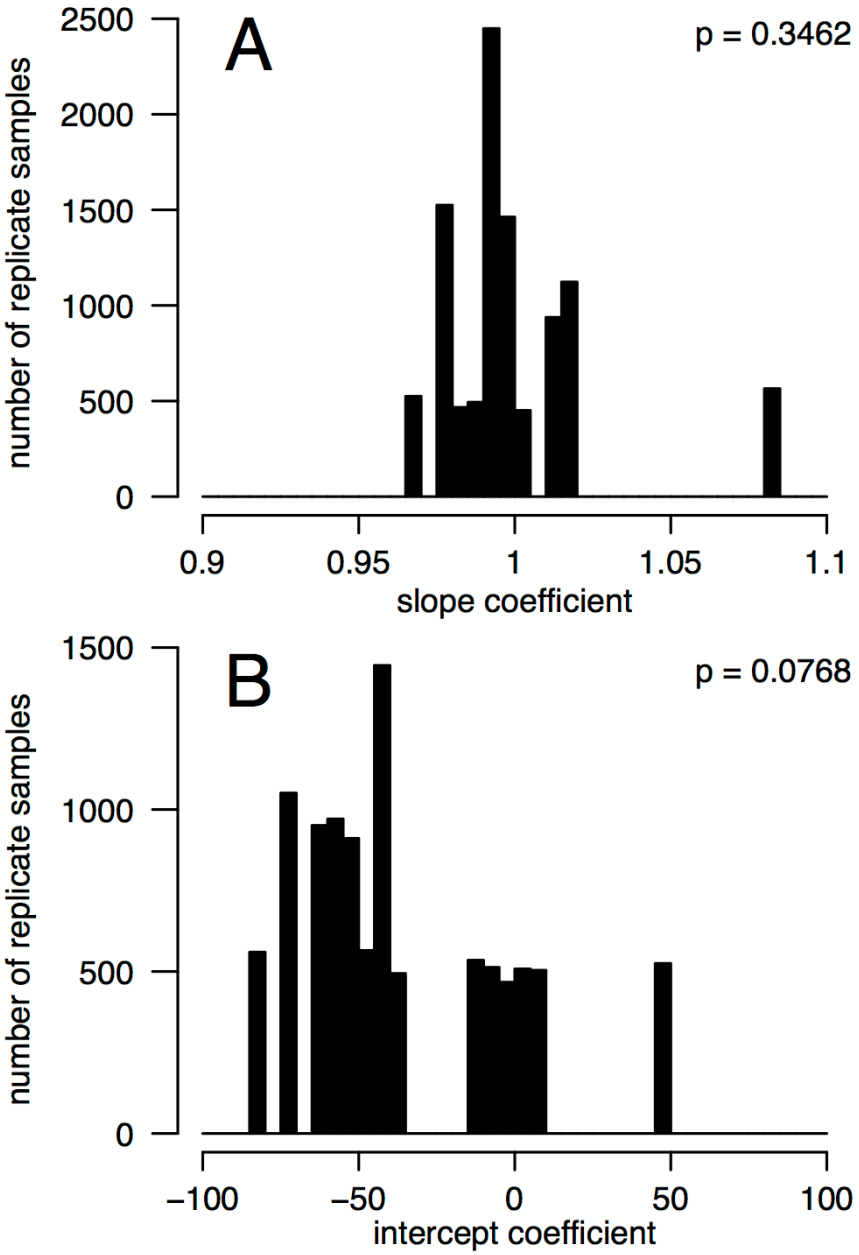

Figure DR2 - Bootstrap-derived sampling distributions of slope and intercept coefficients for reduced major axis regression of graphite versus carbonate targets (see Fig. 1). **A.** Slope coefficient. **B.** Intercept coefficient. Each distribution based on 10,000 replicate bootstrap samples. Symbols: p - two-tailed significance estimates for null hypotheses for slope (b = 1) and intercept (a = 0) coefficients, respectively (based on a percentile approach).

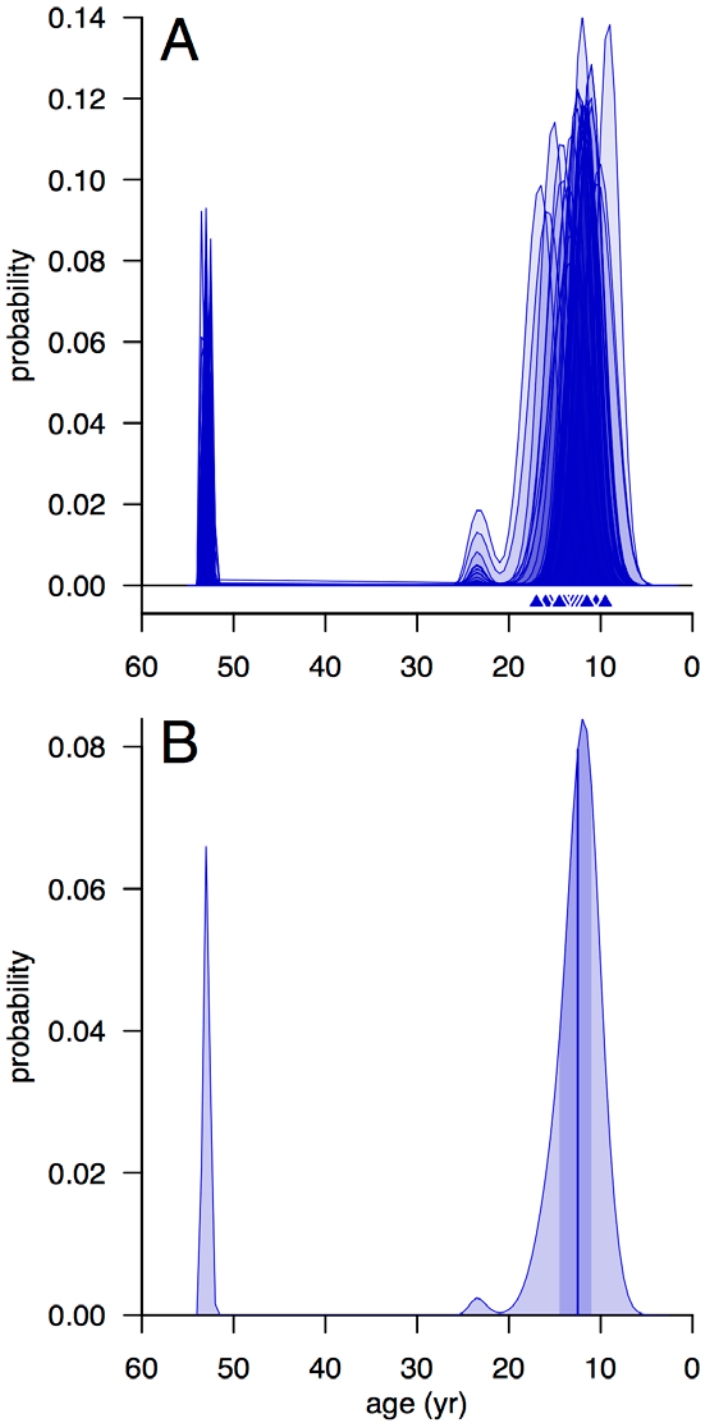

Figure DR3 - Figure 2 panels D&F with x-axis rescaled to 0 to 60 yr. **A.** Individual echinoid calibration posterior distributions from calibration plotted in 10% transparency; triangles at the bottom of the panel indicate median probability ages (Fig. 2B). **B.** Entire combined posterior distribution for echinoids in light blue; inter-quartile age range indicated with darker blue and line indicating median probability age.

References

Baker, M.S., and Wilson, C.A., 2001, Use of bomb radiocarbon to validate otolith section ages of red snapper *Lutjanus campechanus* from the Northern Gulf of Mexico. Limnology and Oceanography v. 46, p. 1819-1824.

Broecker, W.S., and Olson, E.A., 1961, Lamont radiocarbon measurements VIII. Radiocarbon v. 3, p. 176-204.

Bronk Ramsey, C., 2009, Bayesian analysis of radiocarbon dates: Radiocarbon, v. 51, p. 337-360.

Druffel, E.R.M., 1982, Banded corals: changes in oceanic Carbon-14 during the Little Ice Age. Science, v. 218, p. 13-19.

Druffel, E.R.M., 1989, Variability of ventilation in the North Atlantic determined from high precision measurements of bomb radiocarbon in banded corals. Journal of Geophysical Research, v. 94(C3), p. 3271-3285.

Druffel, E.R.M., 1997, Pulses of rapid ventilation in the north Atlantic surface ocean during the past century. Science v. 275, p. 1454-1457.

Druffel, E.R.M., and Linick, T.W., 1978, Radiocarbon in annual coral rings of Florida. Geophysical Research Letters v. 5, p. 913-916.

Fink, D., Hotchkis, M., Hua, Q., Jacobsen, G., Smith, A.M., Zoppi, U., Child, D., Mifsud, C., van der Gaast, H., Williams, A., and Williams, M., 2004, The ANTARES AMS facility at ANSTO. Nucl. Instrum. Methods Phys. Res. B v. 223-224, p. 109-115.

Lighty, R.G., Macintyre, I.G., and Stuckenrath, R., 1982, Acropora palmata reef framework: A reliable indicator of sea level in the Western Atlantic for the past 10,000 years. Coral Reefs v. 1, p. 125-130.

Reimer, P.J., Bard, E., Bayliss, A., Beck, J.W., Blackwell, P.G., Bronk Ramsey, C., Buck, C.E., Cheng, H., Edwards, R.L., Friedrich, M., Grootes, P.M., Guilderson, T.P., Haflidason, H., Hajdas, I., Hatte, C., Heaton, T.J., Hoffmann, D.L., Hogg, A.G., Hughen, K.A., Kaiser, K.F., Kromer, B., Manning, S.W., Niu, M., Reimer, R.W., Richards, D.A., Scott, M.E., Southon, J.R., Staff, R.A., Turney, C.S.M., and van der Plicht, J., 2013, IntCal13 and Marine13 radiocarbon age calibration curves 0-50,000 years cal BP: Radiocarbon, v. 55, p. 1869-1887.

Severinghaus, J.P., Broecker, W.S., Peng, T.-S., and Bonani, G., 1996, Transect along 24^{o}N latitude of ^{14}C in dissolved inorganic carbon in the subtropical North Atlantic Ocean. Radiocarbon v. 38, p. 407-414.